Archival Report

Biological Psychiatry: CNNI

Volatility Estimates Increase Choice Switching and Relate to Prefrontal Activity in Schizophrenia

Lorenz Deserno, Rebecca Boehme, Christoph Mathys, Teresa Katthagen, Jakob Kaminski, Klaas Enno Stephan, Andreas Heinz, and Florian Schlagenhauf

ABSTRACT

BACKGROUND: Reward-based decision making is impaired in patients with schizophrenia (PSZ), as reflected by increased choice switching. The underlying cognitive and motivational processes as well as associated neural signatures remain unknown. Reinforcement learning and hierarchical Bayesian learning account for choice switching in different ways. We hypothesized that enhanced choice switching, as seen in PSZ during reward-based decision making, relates to higher-order beliefs about environmental volatility, and we examined the associated neural activity.

METHODS: In total, 46 medicated PSZ and 43 healthy control subjects performed a reward-based decision-making task requiring flexible responses to changing action–outcome contingencies during functional magnetic resonance imaging. Detailed computational modeling of choice data was performed, including reinforcement learning and the hierarchical Gaussian filter. Trajectories of learning from computational modeling informed the analysis of functional magnetic resonance imaging data.

RESULTS: A 3-level hierarchical Gaussian filter accounted best for the observed choice data. This model revealed a heightened initial belief about environmental volatility and a stronger influence of volatility on lower-level learning of action–outcome contingencies in PSZ as compared with healthy control subjects. This was replicated in an independent sample of nonmedicated PSZ. Beliefs about environmental volatility were reflected by higher activity in dorsolateral prefrontal cortex of PSZ as compared with healthy control subjects.

CONCLUSIONS: Our study suggests that PSZ inferred the environment as overly volatile, which may explain increased choice switching. In PSZ, activity in dorsolateral prefrontal cortex was more strongly related to beliefs about environmental volatility. Our computational phenotyping approach may provide useful information to dissect clinical heterogeneity and could improve prediction of outcome.

Keywords: Bayesian learning, Computational psychiatry, Neuroimaging, Psychosis, Reinforcement learning, Schizophrenia

https://doi.org/10.1016/j.bpsc.2019.10.007

Cognitive and motivational deficits are important characteristics of patients with schizophrenia (PSZ) associated with clinical and social outcomes (1–5). Reward-based learning and decision making require the integration of cognition and motivation and are impaired in PSZ (6,7). These impairments are present at the onset of the disorder, are independent of lower general IQ, remain stable over time (8,9), and have been proposed as neurocognitive markers with potential clinical utility (10). However, the mechanisms and associated neural signatures remain to be identified.

Flexible reward-based learning and decision making can be probed via variants of reversal learning [e.g., (11)]. In such tasks, PSZ show increased switching between choice options (8,12–17). The mechanisms of this unstable behavior remain unknown but can be targeted by computational modeling (18). In reinforcement learning (RL) (19), choices are selected based on expected values, which are learned by weighting reward prediction errors (RPEs) with a learning rate. RPEs closely align with phasic dopamine (20,21). Considering enhanced presynaptic dopamine synthesis capacity in striatum of PSZ (22,23), this could translate into enhanced phasic dopamine in PSZ, which in turn might result in increased learning rates (24). This could theoretically account for unstable behavior in PSZ, but increased learning rates were not found [for reviews, see (18,24,25)].

Theories of predictive coding (26) and hierarchical Bayesian inference hypothesize that symptoms of PSZ (27–29) are a consequence of false inference about the world due to altered precision attributed to beliefs at different hierarchical levels. Dysfunction at higher levels, which are thought to extract and represent general and stable features of the environment, might lead to experiencing the world as being more or less volatile. With regard to positive symptoms (30), this is supported by empirical evidence [e.g., (31)]. When applying this framework to reward-based decision making, beliefs about the probability of rewards are formed at lower levels but are also

ISSN: 2451-9022

determined by learning about the volatility of reward probabilities (32). This environmental volatility is related to learning from lower-level RPEs in that it scales the belief update. Thus, a belief in high environmental volatility can induce rapid updates of lower-level beliefs about reward probabilities and promote enhanced choice switching in PSZ.

Striatal and prefrontal activity is reduced during reward anticipation and receipt in PSZ (33–35). Reduced striatal RPE activity was observed in nonmedicated PSZ (17) but not in medicated PSZ (15,36). Neural correlates of hierarchical Bayesian learning were demonstrated in functional magnetic resonance imaging (fMRI) studies in healthy individuals (37,38), linking volatility and uncertainty to activity in frontostriatal circuits (32,39). While neural correlates of hierarchical Bayesian learning were successfully used to distinguish between individuals with and without hallucinations and PSZ with and without psychosis (31), this has not yet facilitated an understanding of the cognitive and motivational processes underlying impairments in flexible reward-based decision making.

Here, we used a reward-based reversal learning task during fMRI in PSZ and healthy control subjects (HCs). Computational modeling was applied to the behavioral data by comparing RL and a hierarchical Bayesian learning model, the hierarchical Gaussian filter (HGF) (40,41). We hypothesized that enhanced choice switching in PSZ relates to higher-order beliefs about the volatility of the environment and examined the associated neural activity as measured by fMRI.

METHODS AND MATERIALS

Participants and Instruments

In total, 46 medicated PSZ and 43 HCs were included (see Supplemental Table S1). Measures used to characterize participants are summarized in Supplemental Table S1 and the Supplement. Written informed consent was obtained from all participants. The study was performed in accordance with the Declaration of Helsinki and was approved by the local ethics committee of Charité Universitätsmedizin.

Task

Participants performed a task requiring flexible decision making during fMRI (42–44). The task had 160 trials, each with a choice between two cards (Figure 1A). The selected card resulted in a monetary win or a monetary loss of 10 Eurocents. One card was initially assigned with a reward probability of 80% and a loss probability of 20% (vice versa for the other card). The task had a simple higher-order structure (Figure 1B): an anticorrelation between the reward probabilities; whenever one card was associated with a probability of 80%, the other card would be associated with a probability of 20%. Reward contingencies were stable for the first 55 trials (pre-reversal) and for the last 35 trials (post-reversal). During the reversal phase, contingencies changed four times after 15 or 20 trials. For more details, see Supplement.

Analysis of Choice Behavior

Performance was quantified by correct choices of the stimuli with high (80%) reward probability and was analyzed using repeated-measures analysis of variance (ANOVA) with the between-subject factor group and the within-subject factor phase (pre-reversal, reversal, or post-reversal). Repeated-measures ANOVA was used to test the effect of feedback on subsequent choices (win–stay and lose–stay).

Computational Models of Learning

In RL, the difference between received rewards and expectations, the RPE, is used to update expectations for the chosen stimulus (weighted by the learning rate α). For comparison with previous work (17,42–44), we included RL with separate learning rates for reward and loss trials (RL1 and RL2).

The HGF describes learning as a process of inductive inference under uncertainty. It considers hierarchically organized states in which learning at a higher-level state determines learning at a lower-level state by dynamically adjusting the lower level's learning rate. In our case, the top level represents environmental volatility (how likely a change in

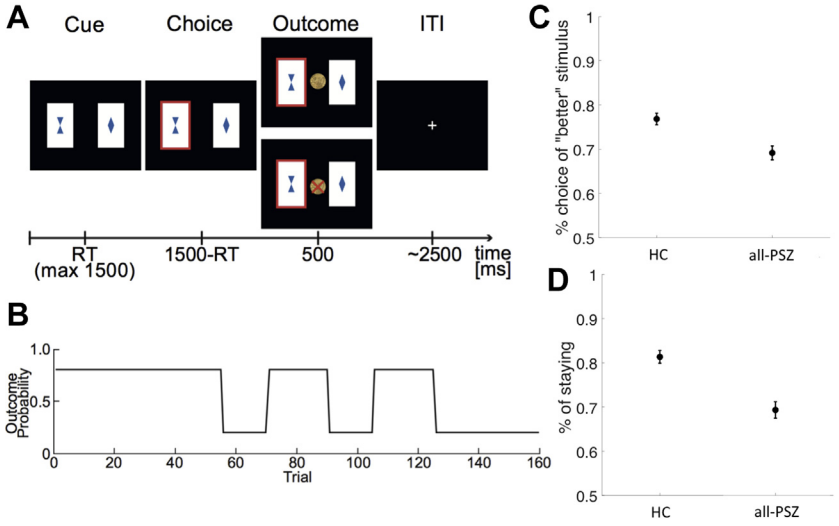

Figure 1. **(A)** Trial sequence from the decision-making task. **(B)** Reward probabilities of both choice options were perfectly anticorrelated and were stable for the first 55 trials (pre-reversal); changed 4 times, after 15 or 20 trials, during the reversal phase; and remained stable for the last 35 trials (post-reversal). **(C)** Percentage choices of the stimulus with 80% reward probability were significantly lower in the patients with schizophrenia (PSZ) group (main effect of group, $F = 14.52$, $p < .001$). **(D)** PSZ were less likely to repeat the previous action independent of feedback received in the previous trial (main effect of group, $F = 27.77$, $p < .001$; feedback × group interaction, $F = 0.02$, $p = .89$). HCs, healthy control subjects; ITI, intertrial interval; RT, reaction time.

action–outcome contingencies is to occur). This top-level estimate is dynamically coupled with learning at the lower level (see Figure 2). Trial-by-trial updates of posterior means at each level are proportional to the prediction error (PE) from the level below weighted by a precision ratio. See Supplement for equations. We were particularly interested in environmental volatility (μ_3) and its coupling with the lower level (κ) and thus inferred subject-specific parameters. We included a 2-level variant (HGF2) to test whether the representation of volatility in the 3-level HGF3 made it superior in explaining behavior.

HGF and RL provide different ways to learn expectations about rewards, and both update expectations of the chosen card only (single update [SU]). Based on the anticorrelated task structure, we implemented a variant of each model updating values (RL) or posterior means (HGF) of the unchosen card simultaneously; that is, an increase of the chosen card implies a decrease of the unchosen card (double update [DU]). For equations, see Supplement. SU and DU variants of each model (RL1, RL2, HGF2, and HGF3) were fit to the choice data (Table 1).

Decision Models

Values (RL) or posterior means (HGF) were transformed to choice probabilities by using the softmax (logistic sigmoid) function (see Supplement). In binary choice tasks with anticorrelated reward probabilities such as ours, there is choice perseveration independent of learning or inference that differs between win and loss trials. We captured this by estimating parameters for win and loss trials that reflect this difference in choice perseveration (ρ_{win} and ρ_{loss}). Models that included inverse decision noise β as a free parameter had lower evidence (see Supplement) than models where this was fixed to unity ($\beta = 1$). We also tested the possibility that volatility is directly linked to choice probabilities by letting third-level trial-by-trial volatility (HGF3) serve as the inverse decision noise (see Supplement). Because this introduced a volatility scale anchored in observed behavior (switching or staying), it allowed for estimating the mean of the subjective a priori belief about initial volatility at the third level, $\mu_3^{(0)}$, as a parameter of HGF3. This cannot be applied to RL and HGF2 because they do not feature inference on volatility. This led to 2 additional models (HGF3-SU-V and HGF3-DU-V), resulting in a total of 10 models. For model fitting, see Supplement.

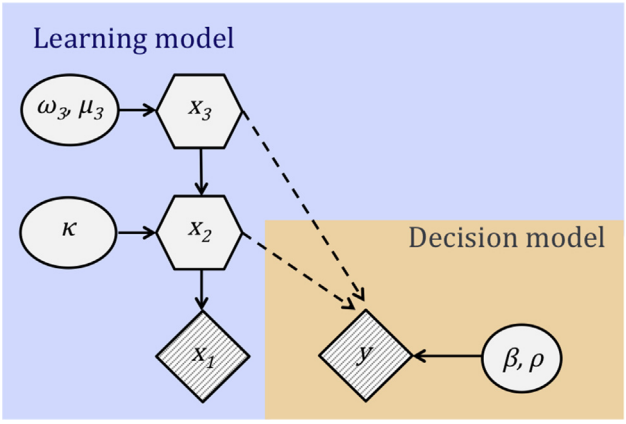

Figure 2. Model graph. The hierarchical Gaussian filter deploys hierarchically organized states in which learning about environmental volatility at a higher-level state x_3 determines lower-level learning about reward probabilities x_2. The lowest level, x_1, is binary and corresponds to a choice being rewarded ($x_1 = 1$) or not ($x_1 = 0$) at a given trial. The probability of a choice being rewarded is a logistic sigmoid function of x_2: $p(x_1 = 1) = s(x_2)$. y represents the response of the subject. Shaded quantities are observed. Solid lines indicate dependence in the generative model. Dashed lines indicate dependence on inferred quantity (the generative model for y depends on μ_2 and μ_3, the inferred values of x_2 and x_3, respectively). The constant step size ω_3 is the evolution rate of environmental volatility. κ reflects the coupling between the levels. The best-fitting model was a three-level implementation (HGF3-DU-V) with double updating (not illustrated) together with a decision model capturing choice repetition separately after rewards and losses (ρ), third-level environmental volatility determining decision noise, and the initial belief about environmental volatility μ_3 as an additional parameter inferred from the data. DU, double update; HGF, hierarchical Gaussian filter; V, environmental volatility.

Model Selection

The negative variational free energy (an approximation to the log model evidence) was used for random-effects Bayesian model selection (45). The protected exceedance probability (PXP) governed our model selection, which protects against the null possibility that there are no differences in the likelihood of models across the population (46). We also examined whether the models explained the data better than chance (17,47). A subject was classified as not fit better than chance if the log likelihood of the data relative to the number of trials did not significantly differ from chance (see Supplemental Methods). Simulations of the task were run using the inferred parameters to reproduce the observed data.

Model Parameters

Parameters of the winning model were compared between groups using *t* test or the nonparametric Mann-Whitney *U* test if assumptions of normality were violated (Kolmogorov-Smirnov test). Bonferroni correction was applied according to the number of parameters.

Statistical Analysis of fMRI Data

Using the general linear model approach in SPM8, an event-related analysis was applied. On the first level, 1 regressor spanned the entire trial from cue to outcome as in a previous study (38). We added the following 5 modeling-based trajectories as parametric modulators (not orthogonalized) to best capture different aspects of the hierarchical inference process: second- and third-level precision-weighted PEs (ε_2 and ε_3), which were time locked to the outcome, precision weights (ψ_2 and ψ_3), and the third-level volatility (μ_3). All regressors spanned the entire trial and changed at outcome accordingly to PE updates identical to Iglesias *et al.* (38). Regressors were convolved with the canonical hemodynamic response function in SPM8 and its temporal derivative (see Supplemental Methods). For second-level analysis, a random-effects ANOVA model, including contrast images of the 5 modeling-based trajectories (precision-weighted PEs [ε_2 and ε_3], precision weights [ψ_2 and ψ_3], and the third-level volatility [μ_3]) and the factor group, was estimated.

Table 1. Bayesian Model Selection

		RL1-SU	RL1-DU	RL2-SU	RL2-DU	HGF2-SU	HGF2-DU	HGF3-SU	HGF3-DU	HGF3-SU-V	HGF3-DU-V
HCs + PSZ All (n = 89)	PP	9.4	5.1	7.4	3.0	3.1	7.0	3.3	7.7	5.3	48.8
	XP	0	0	0	0	0	0	0	0	0	100
	PXP	0	0	0	0	0	0	0	0	0	99.9
HCs All (n = 43)	PP	4.4	4.7	4.4	3.8	2.7	5.1	2.7	5.3	5.8	61.1
	XP	0	0	0	0	0	0	0	0	0	100
	PXP	0	0	0	0	0	0	0	0	0	100
PSZ All (n = 46)	PP	11.8	7.1	11.6	4.75	8.3	10.0	9.3	10.9	4.9	21.4
	XP	6.9	0.7	6.21	0.1	1.4	3.4	2.5	4.6	0.2	74.0
	PXP	10.0	10.0	10.0	10.0	10.0	10.0	10.0	10.0	10.0	10.1
HCs + PSZ Fit (n = 73)	PP	9.4	5.1	7.4	3.0	3.2	6.9	3.3	7.7	5.3	48.8
	XP	0	0	0	0	0	0	0	0	0	100
	PXP	0	0	0	0	0	0	0	0	0	100
HCs Fit (n = 42)	PP	4.5	4.5	4.5	3.8	2.8	5.3	2.8	5.5	5.8	60.5
	XP	0	0	0	0	0	0	0	0	0	100
	PXP			0	0	0	0	0	0	0	100
PSZ Fit (n = 31)	PP	11.6	8.2	11.3	4.9	7.9	9.7	8.9	10.4	4.9	22.3
	XP	5.5	1.1	4.8	0.1	1.0	2.5	1.7	3.3	0.1	80.0
	PXP	10.0	10.0	10.0	10.0	10.0	10.0	10.0	10.0	10.0	10.1

Bayesian model selection was governed by protected exceedance probabilities (PXPs) to protect against the risk that differences in model evidence occur by chance. In this table, we also report exceedance probabilities (XPs) and expected posterior probabilities (PPs); also see the Supplement. XP describes the probability of a model exceeding all other models in the comparison set, the probability that expected PPs differ.

DU, double update; HCs, healthy control subjects; HGF, hierarchical Gaussian filter with 2 or 3 levels; HGF3-**-V, 3-level HGF with environmental volatility linked to decision noise with either SU or DU; PSZ, patients with schizophrenia; RL, reinforcement learning with one learning rate (RL1) or separate learning rates for rewards and losses (RL2); SU, single update.

RESULTS

Behavioral Data

Repeated-measures ANOVA on correct choices showed that performance differed between phases, dropping during the reversal phase (main effect of phase, $F = 23.74$, $p < .001$). PSZ chose the better card less frequently irrespective of task phases (main effect of group, $F = 14.52$, $p < .001$, and phase × group interaction, $F = 1.87$, $p = .16$) (Figure 1C). The factor phase was dropped from further analyses.

Repeated-measures ANOVA on the probability of choice repetition showed that all participants stayed more with the previous action after rewards compared with losses (main effect of feedback, $F = 369.80$, $p < .001$) and that PSZ switched more independent of feedback from the previous trial (main effect of group, $F = 27.77$, $p < .001$, and feedback × group interaction, $F = 0.02$, $p = .89$) (Figure 1D).

Computational Modeling: Model Selection

Random-effects Bayesian model selection revealed a 3-level HGF with double updating and third-level environmental volatility linked to decision noise (Figure 2) as the most plausible model (HGF3-DU-V, PXP = 99.5%; for PXPs of all models, see Table 1). This model (HGF3-DU-V) was superior in HCs (PXP = 100%, Bayes omnibus risk = 0) and remained first ranking in PSZ (posterior probabilities = 21.4%, PXP = 74.0%). In PSZ, there was no convincing evidence that models performed differently from each other (Bayes omnibus risk = 1, all PXPs = 10.0%).

In total, 15 PSZ and 1 HCs were not fit better than chance by any model (Figure 3A). Neither when considering all PSZ (PSZ-fit + PSZ-nofit) nor when considering PSZ-fit alone did Bayesian model selection reveal a clearly superior model (both times Bayes omnibus risk = 1) (Table 1). However, the identification of PSZ-fit ensures that individuals included in further modeling-based analyses are fit better than chance by every model (i.e., equally good models instead of equally poor models).

Revisiting Behavioral Data

Based on this heterogeneity in PSZ regarding absolute model fit, we revisited choice data with respect to 3 groups (HCs, PSZ-fit, and PSZ-nofit). There was a main effect of group on correct choices ($F = 32.63$, $p < .001$) (Figure 3B). PSZ-nofit showed performance around chance levels (HCs vs. PSZ-nofit, $t = 7.04$, $p < .001$; PSZ-fit vs. PSZ-nofit, $t = 6.90$, $p < .001$) (Figure 3B), while PSZ-fit had performance comparable to HCs ($t = 1.51$, $p = .14$) (Figure 3B). The analysis of win–stay and lose–stay behavior revealed a group × feedback interaction ($F = 20.68$, $p < .001$). This resulted from a pronounced reduction of win–stay behavior in PSZ-nofit only (PSZ-fit vs. PSZ-nofit, $t = 10.74$, $p < .001$) (Figure 3C), while reduced lose–stay was not significantly different between PSZ-fit and PSZ-nofit ($t = 0.01$, $p = .99$) (Figure 3D). A group × feedback interaction was also significant when comparing only HCs and PSZ-fit ($F = 6.79$, $p = .01$) as well as significant main effects of feedback ($F = 636.30$, $p < .001$) and group ($F = 10.22$, $p = .01$). This difference between HCs and PSZ-fit was driven by switching after loss (Figure 3C, D).

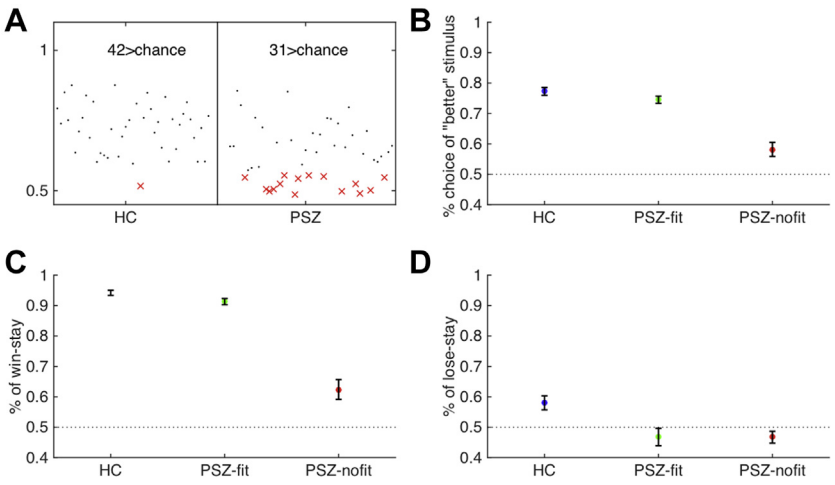

Figure 3. **(A, B)** Classification above (black dots) and below (red crosses) chance **(A)** and its influence on overall choice performance **(B)**. There was a main effect of group ($F = 32.63$, $p < .001$). Patients with schizophrenia (PSZ)-nofit (red) showed overall poor performance (healthy control subjects [HCs] vs. PSZ-nofit, $t = 7.04$, $p < .001$; PSZ-fit vs. PSZ-nofit, $t = 6.90$, $p < .001$), while PSZ-fit (green) performed comparably to HCs (blue) ($t = 1.51$, $p < .14$) **(B)**. **(C, D)** Analysis of win–stay **(C)** and lose–stay **(D)** behavior showed a group × feedback interaction ($F = 20.68$, $p < .001$). There was a pronounced reduction of win-stay behavior in PSZ-nofit only (PSZ-fit vs. PSZ-nofit, $t = 10.74$, $p < .001$) **(C)**, while reduced lose-stay behavior characterized both groups of PSZ (PSZ-fit vs. PSZ-nofit, $t = 0.01$, $p = .99$) **(D)**. This group × feedback interaction was also significant when comparing only HCs and PSZ-fit.

In an exploratory analysis of 6 cognitive tests, only measures of verbal memory and working memory differed between the 2 groups of PSZ, that is, were more impaired in PSZ-nofit compared with PSZ-fit (see Supplemental Results). This suggests that PSZ-fit and PSZ-nofit mapped on distinct cognitive profiles. Because poor fit hinders the interpretation of modeling-based behavioral and neuroimaging analyses in the PSZ-nofit subgroup, all subsequent modeling-based results are reported based on HCs ($n = 42$) and PSZ-fit ($n = 31$) only.

Computational Modeling: Parameters

Comparison of parameters of HGF3-DU-V (Table 2 and Figure 4) revealed that the estimated mean of the a priori belief about initial environmental volatility $\mu_3^{(0)}$ was higher in PSZ ($z = 3.15$, $p < .01$) (Figure 4A). Trial-by-trial environmental volatility was more strongly coupled with lower-level updating, as demonstrated by higher κ in PSZ ($z = 2.51$, $p < .01$) (Figure 4B). The evolution rate of environmental volatility ω_3 did not differ significantly between groups ($z = 0.73$, $p = .47$). To illustrate the effects of differences in parameters on behavior after losses (when PSZ-fit showed increased switching), we analyzed the trajectory of μ_3 in a mixed-effects regression model with group and feedback as predictors. This revealed higher μ_3 in PSZ-fit overall. Across groups, μ_3 was higher after losses compared with rewards, which was more pronounced in PSZ (resulting from enhanced coupling between higher and lower levels of κ). For statistics, see Supplemental Results and Supplemental Figure S2.

Computational Modeling: Reproducing Observed Behavior

Simulating data based on the inferred parameters of HGF3-DU-V (42 HCs, 31 PSZ-fit, 10 simulations per subject) showed that PSZ-fit switched more than HCs (main effect of group, $F = 11.17$, $p < .001$) and showed a pronounced tendency to switch after losses (group × feedback, $F = 7.68$, $p = .01$). Between-group findings on behavioral data were fully reproduced, which yields an important validation of the model's ability to capture the observed data.

Computational Modeling: Replication in Nonmedicated PSZ

We tested our model (HGF3-DU-V) in an independent sample of nonmedicated PSZ ($n = 24$) and HCs ($n = 24$), who performed another reversal-learning task (17). For statistics, see Table 2. This replicated between-group findings and remained significant when excluding participants not fit better than chance (23 HCs, 13 PSZ; not reported).

Relation to Symptoms

We explored the relation between the 2 parameters that differed between groups with different measures of cognition ($n = 6$) and clinical measures ($n = 7$) within PSZ (Supplemental Table S1) applying Bonferroni correction ($p < .0083$). In PSZ, a higher initial belief about volatility $\mu_3^{(0)}$ was associated with reduced executive functioning and cognitive speed (Trail Making Test B: $r = -.56$, $p < .001$; Digit Symbol Substitution Test: $r = -.56$, $p < .001$) (Supplemental Table S3 and Supplemental Figure S3). These correlations were not present in the HC group. For all explorative correlations, see Supplemental Table S3.

fMRI Task Effects (Pooled Across Groups)

Activity related to ε_2 (a precision-weighted RPE) peaked in bilateral ventral striatum and ventromedial prefrontal cortex (PFC) among other regions ($p\text{-FWE}_{\text{wholebrain}} < .05$, where FWE is familywise error) (Figure 5A and Supplemental Table S4), including the midbrain ($p\text{-FWE}_{\text{midbrain-voi}} < .05$, where voi is volume of interest) (Supplemental Table S9), a well-known network associated with RPEs. In contrast, third-level precision-weighted PE (ε_3) was associated with activity in prefrontal, parietal, and left insular regions (Figure 5A and Supplemental Table S5). Environmental volatility (μ_3) covaried with activation in bilateral insula, cingulate cortex, parietal cortex, middle temporal gyrus, globus pallidus, and thalamus as well as superior, middle, and inferior frontal gyrus (Figure 6A, Supplemental Figure S5, and Supplemental Table S8). For more details on group-level fMRI effects, including activity

Table 2. Between-Group Comparisons of Model Parameters Using *t* Tests or the Nonparametric Mann-Whitney *U* Test If Assumptions of Normality Were Violated

Models	HCs (n = 42)	PSZ (n = 31)	Test Statistic
Learning Model			
μ_3	−0.84 ± 0.49	−0.47 ± 0.48	$z = 3.15$, $p < .01$
κ	0.87 ± 0.60	1.35 ± 1.12	$z = 2.51$, $p < .01$
ω_3	−6.00 ± 0.02	−5.99 ± 0.05	$z = 0.73$, $p = .47$
Decision Model			
ρ_{win}	0.97 ± 0.57	1.08 ± 0.49	$z = 0.88$, $p = .38$
ρ_{loss}	0.08 ± 0.31	−0.12 ± 0.44	$z = 2.37$, $p = .02$
	Replication Sample[a]		
	HCs (n = 24)	Nonmedicated PSZ (n = 24)	Test Statistic
Learning Model			
μ_3	−1.17 ± 0.61	−0.43 ± 0.70	$z = 3.88$, $p < .01$
κ	0.61 ± 0.58	1.56 ± 1.21	$z = 3.46$, $p < .01$
ω_3	−6.09 ± 0.02	−5.99 ± 0.06	$z = 1.35$, $p = .18$
Decision Model			
ρ_{win}	0.70 ± 0.74	0.43 ± 0.66	$z = 1.35$, $p = .18$
ρ_{loss}	−0.07 ± 0.59	−0.28 ± 0.77	$z = 1.05$, $p = .30$

Bonferroni correction was applied according to the number of parameters (5) ($p < .01$).
HCs, healthy control subjects; PSZ, patients with schizophrenia.
[a]Schlagenhauf *et al*. (17).

specific for each group outside the effect of each regressor combined for HCs and PSZ, see Supplemental Results.

fMRI Between-Group Effects

We conducted between-group comparison of the covariance between the modeling regressors derived from the best-fitting model and blood oxygen level–dependent response within SPM. For the regressor of environmental volatility μ_3, a group difference between HCs and PSZ was found in right dorsolateral PFC (DLPFC) (*F* contrast, using a mask representing the average effect of μ_3 over all participants for correction of multiple comparison [x = 34, y = 44, z = 24], $F = 19.89$, $z = 4.24$, $p_{FWE} = .04$) (Figure 6B). Post hoc analysis revealed stronger activity related to volatility in DLPFC of PSZ compared with HCs ($t = 4.46$, $z = 4.4$, $p_{FWE} = .02$) (Figure 6C). There was no significant difference between groups for any other regressor.

DISCUSSION

To the best of our knowledge, this is the first study to apply hierarchical Bayesian learning to choice and fMRI data of PSZ during reward-based decision making. We present two main findings. First, our modeling suggests that medicated PSZ acted under an a priori enhanced higher-level belief about initial environmental volatility and increased coupling between higher and lower levels of learning, which leads to enhanced lower-level belief updating about action–outcome contingencies. This provides a computational account of choice switching, as was previously observed in PSZ (8,12–17). Using parameters of the winning model to simulate new data, we fully reproduced observed patterns in the behavioral data, and we replicated our findings on parameters in an independent cohort of nonmedicated PSZ. Second, medicated PSZ displayed higher DLPFC activity related to environmental volatility, which points toward a prominent role of this region in promoting unstable behavior in PSZ.

PSZ show enhanced choice switching (8,12–17), and we demonstrate a possible underlying mechanism: an enhanced initial belief about the environmental volatility and a stronger coupling of volatility and lower-level learning of action–outcome contingencies. This has two consequences. First, PSZ had an overall stronger tendency to switch (enhanced initial belief about volatility). Second, lower-level beliefs fluctuated more strongly and

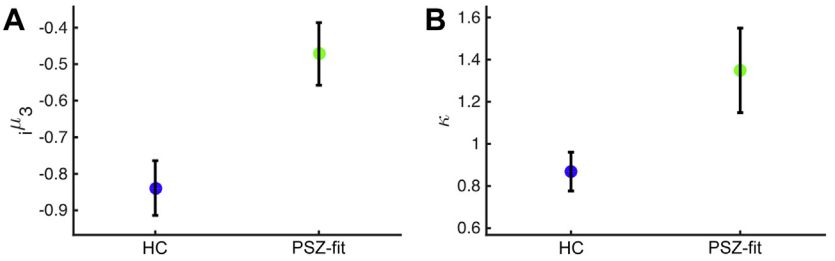

Figure 4. **(A)** The initial estimate of environmental volatility is significantly higher in patients with schizophrenia (PSZ)-fit (n = 31) as compared with healthy control subjects (HCs). **(B)** The coupling between the third level (environmental volatility) and the second level is significantly stronger in PSZ-fit (n = 31) compared with HCs.

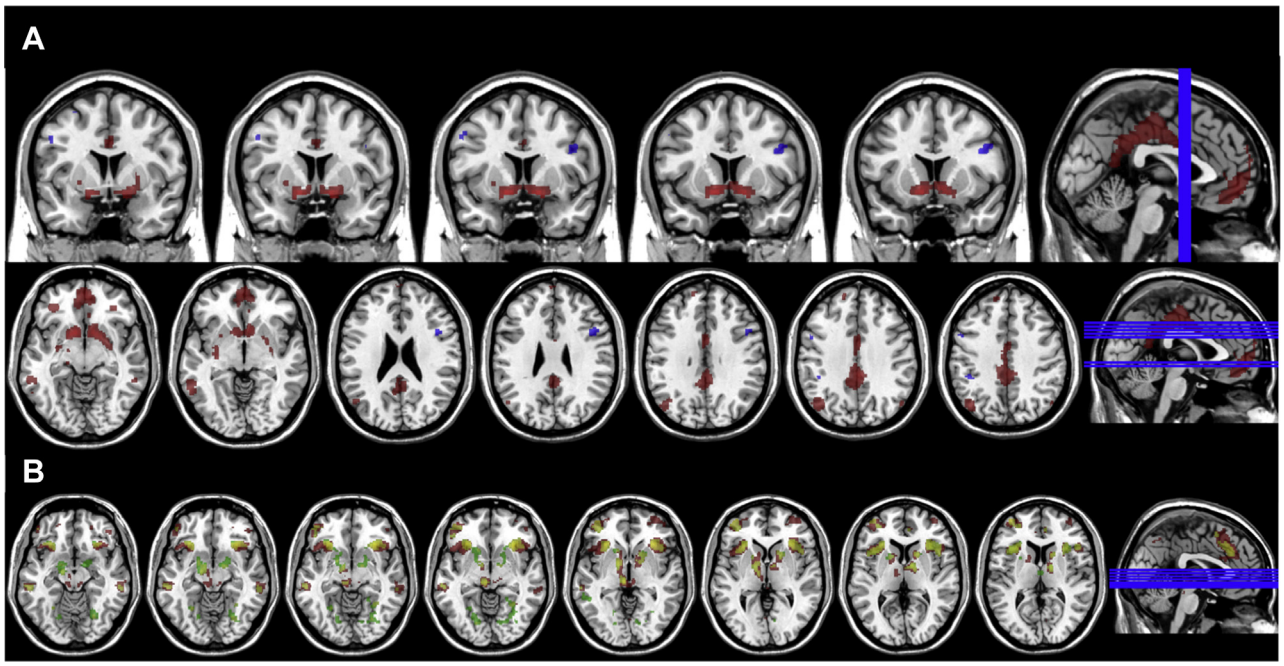

Figure 5. Blood oxygen level–dependent signal across all participants related to precision-weighted prediction errors from the second (red) and third (blue) levels **(A)** and precision weight from the second (red) and third (green) levels **(B)**, with overlap in yellow (both at $p\text{-FWE}_{\text{wholebrain}} < .05$, $k = 10$). FWE, familywise error.

led to increased choice switching, particularly after (irrelevant) losses. Thus, PSZ inferred more contingency changes in this dynamic task environment that are putatively signaled through losses. Enhanced estimates of changes in context probabilities were also found in PSZ in the nonreward domain (48). In contrast to our finding of enhanced initial belief about volatility, Powers *et al.* (31) probed conditioned hallucinations and reported stronger lower-level priors about perceptual inputs combined with reduced evolution of volatility in hallucinating participants. A possible explanation may be that alterations of volatility estimates differ with regard to the investigated functional domain, potentially related to different symptom dimensions. As suggested by our finding, cognitive beliefs about the structure of the environment appear to be more unstable, while perceptual beliefs about sensory inputs appear to be overly stable and not appropriately adjusted following changes in the environment (31).

Because our model revealed consistent results in medicated and nonmedicated PSZ, elevated beliefs about environmental volatility may represent an important mechanism of impaired flexible decision making. In a similar vein, an inability to stabilize behavior according to an internal model of action–outcome contingencies was found after administration of ketamine in healthy control subjects (49), in line with the assumption that reduced (prefrontal) NMDA receptor functioning (27,50) may lead to aberrant cortical information processing (51). In line with this idea, we found a stronger association in PSZ than in HCs of beliefs about volatility with blood oxygen level–dependent activity in DLPFC. However, in our fMRI study, we cannot infer about involved neurochemical systems. On the behavioral level, beliefs about higher volatility, in our model directly linked to decision noise, can lead to more stochastic behavior (in our task overall more choice switching). We therefore suggest that heightened neural representation of volatility may generate more stochastic behavior, although in our correlational and cross-sectional study we cannot ascertain a causal link. We found a negative correlation of the initial belief about volatility with independent neuropsychological measures of executive functioning and cognitive speed in PSZ, thereby emphasizing its dysfunctional character, while these associations were not observed in the HC group.

PSZ's heightened belief about volatility may render a system (hyper)sensitive to any new input (51,52), thereby impeding the detection of regularities in probabilistic environments and leading to (hyper)flexible updating in response to (irrelevant) information. Meta-analyses showed reduced prefrontal activity in PSZ compared with HCs for (relevant) task versus (irrelevant) conditions across multiple cognitive measures (53,54). On the one hand, prefrontal dysfunction in PSZ may contribute to an enhanced higher-level belief about volatility (e.g., by impairing the detection of higher-level regularities), and such beliefs about volatility might be assigned with enhanced precision (potentially in a compensatory manner). On the other hand, lower-level beliefs may be more unstable and presumably assigned with lower precision, leading to distinct aberrant experiences and behaviors depending on the tested domain, with most evidence so far coming from perceptual processing (55).

Aberrant cortical processing was theorized, at least in nonmedicated PSZ, to increase striatal dopamine turnover (27,50), which might interfere with striatal and midbrain RPE signals. Indeed, in nonmedicated PSZ, striatal RPE activity was found to be reduced (17,56). In RL accounts (24), enhanced spontaneous phasic dopamine transients could highlight irrelevant stimuli and disturb the signaling of (relevant) RPEs. In our medicated sample of PSZ, no significant differences in striatal activations to RPEs

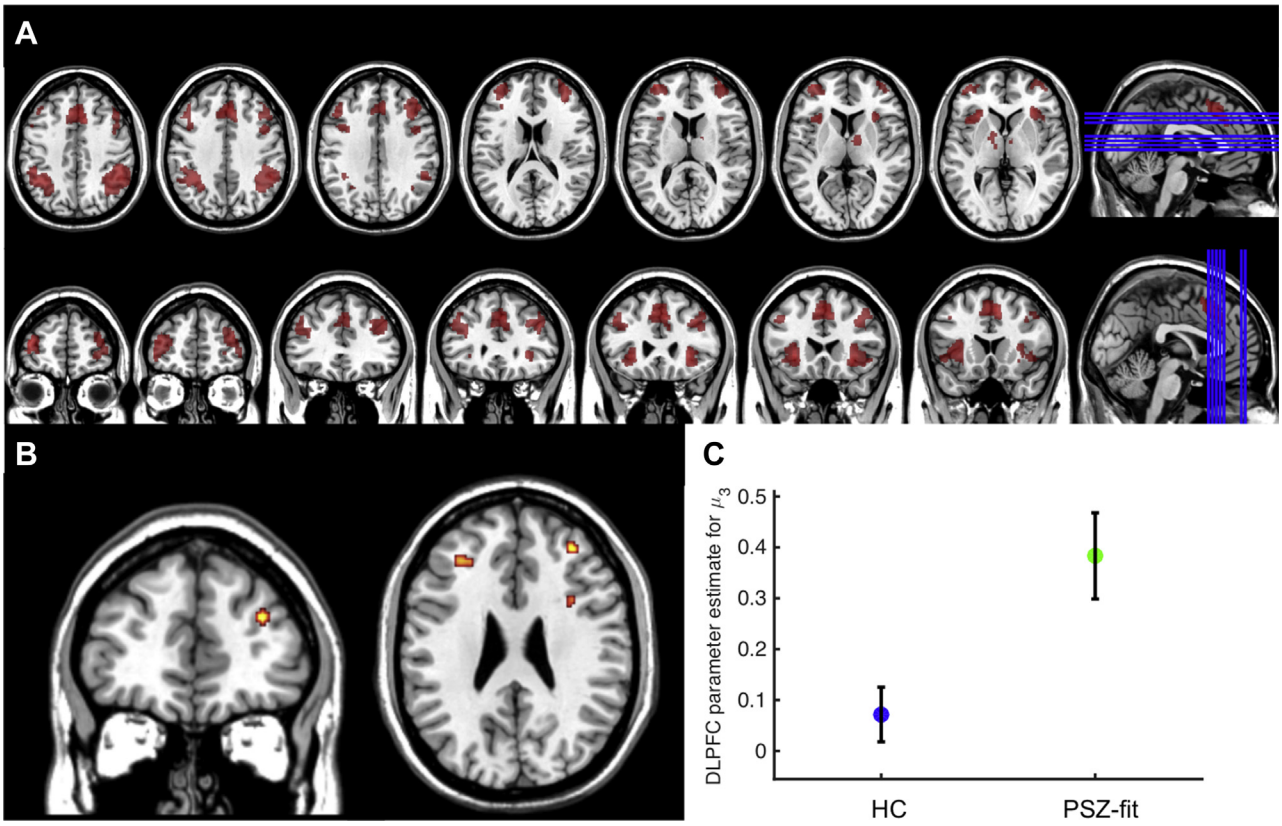

Figure 6. **(A)** Across all participants, blood oxygen level–dependent signal related to volatility estimate from the third level at p-FWE $< .05$ for the whole brain, $k = 10$. **(B)** μ_3-related blood oxygen level–dependent signal in the dorsolateral prefrontal cortex (DLPFC) differs between patients with schizophrenia (PSZ)-fit ($n = 31$) and healthy control subjects (HCs) (F contrast displayed at $p < .001$ uncorrected; corrected for main effect of μ_3 over all participants [x = 34, y = 44, z = 24], $F = 19.89$, $z = 4.24$, $p = .038$). **(C)** A post hoc analysis of regression parameter estimates at the peak of the group difference (x = 34, y = 44, z = 24) showed that this was driven by heightened activation related to environmental volatility in DLPFC of PSZ-fit ($n = 31$) compared with HCs ($t = 4.46$, $z = 4.4$, $p = .019$). FWE, familywise error.

were observed, in line with reports of absent differences in striatal RPEs in medicated PSZ (14,15). This suggests medication status as an important factor relating to striatal RPE signaling similar to medication effects on striatal reward anticipation in PSZ (35,57,58). In hierarchical Bayesian learning, representation of lower-level PEs may be similar in patients and control subjects, but potentially reduced precision of lower-level beliefs might highlight irrelevant inputs (e.g., resulting in choice switching). This could, at least in theory, result from a common aberrant prefrontal process, as discussed above, but also from an effect of antipsychotic D_2 receptor antagonists in the striatum (29). However, we did not observe group differences in midbrain and striatum for precision weights and precision-weighted PEs. While our data indicate a disrupted higher-level process with evidence from behavioral modeling and fMRI, disturbed lower-level processes are supported by our behavioral modeling but not by the presented fMRI data.

Limitations

First, the lack of clear superiority of any model for the data from PSZ, as well as the substantial number of PSZ in which no model fitted better than chance, needs to be considered. Excluding these patients from further modeling-based analyses can be considered restrictive and may reduce the generalization of results. However, 2 subgroups were identified with (task-independent) different cognitive profiles, which contributes to disentangling heterogeneity across PSZ—a fundamental challenge for psychiatric research (59). By controlling whether subjects' performance can actually be interpreted as assumed by the theories, we eliminated a potential key confound. Nevertheless, it remains problematic if clinical groups differ in how well they are described by models of interest, as observed in our study because parameters are conditional on the model. This impedes the interpretation of differences in parameters across groups [for a discussion of this problem, see (60)]. In principle, Bayesian model averaging (61) can help, but this is not established for non-nested models as used here. Future studies might implement tasks with adaptive difficulty to reduce the number of patients whose behavior cannot be explained by any model, which may potentially be a result of excessive cognitive demands. Furthermore, the relation between different Bayesian modeling approaches such as the HGF and active inference models should be explored (62).

Second, we suggest that overestimating volatility is one possible explanation for choice switching. However, in our model, volatility partly determines decision noise. This limits the differentiation between the concepts of volatility and

exploration and limits interpretability of volatility estimates to some extent. The finding that this model performs best is an indication that our data do not fully support a strong distinction between volatility and exploration. Additional task-based manipulations would be required to overcome this (37), which would most likely involve longer tasks than our patient-friendly fMRI task (<15 minutes, 160 trials). The formulation of our response model suggests that results are still informative. We control for overall differences in stickiness with 2 parameters that change the shape of the decision function differently for wins and losses and exert a bias toward repeating or switching responses irrespective of learned expectations (see Supplement). Therefore, decision noise is determined not only by trialwise volatility but also by subject-specific traits that are expressed in a condition-specific fashion. This disentangles volatility and decision noise to some degree.

Third, this is a case-control study that fundamentally limits the inferences that can be drawn from the results, for example, the development of inappropriately high initial beliefs about volatility over the course of illness, its stability over time, and its relation to broader cognitive deficits consistently found in PSZ.

In summary, we present a computational mechanism putatively underlying unstable behavior in PSZ: a stronger coupling of heightened beliefs about environmental volatility with lower-level learning, which was present in medicated and nonmedicated PSZ. In medicated PSZ, this was accompanied by enhanced activity related to environmental volatility in DLPFC. Future studies should aim to test specificity of the presented results for PSZ and overcome the limitation of the lack of longitudinal clinical data. Computational modeling may aid in the identification of subgroups of PSZ (63) and potentially inform the prediction of treatment response to antipsychotic drugs by aiming to dissect the important biological heterogeneity and interindividual differences among patients (64). These steps toward clinically useful procedures will require carefully designed prospective studies in the framework of computational psychiatry (29,65–67).

ACKNOWLEDGMENTS AND DISCLOSURES

This study was supported by the Max Planck Society and grants from the German Research Foundation (Grant Nos. DFG SCHL1969/1-2, DFG SCHL 1969/3-1, and DFG SCHL1969/4-1 [to FS]). JK is supported by the Charité Clinician-Scientist Program of the Berlin Institute of Health. KES acknowledges support by the René and Susanne Braginsky Foundation and the University of Zurich.

LD, CM, KES, and FS designed the study. LD, RB, TK, and JK performed research. LD and RB analyzed the data. CM and FS supervised data analysis. LD and RB wrote the initial version of the manuscript. LD, RB, TK, JK, CM, KES, AH, and FS read and corrected versions of the manuscript.

Data from this study were presented at the following conferences: 71st annual meeting of the Society for Biological Psychiatry, May 12–14, 2016, Atlanta, Georgia; 6th biennial Schizophrenia International Research Society Conference, April 4–8, 2018, Florence, Italy; and 11th Forum of Neuroscience, July 7–11, 2018, Berlin, Germany.

All authors report no biomedical financial interests or potential conflicts of interest.

ARTICLE INFORMATION

From the Department of Psychiatry and Psychotherapy (LD, RB, TK, JK, AH, FS), Charité Universitätsmedizin Berlin, corporate member of Freie Universität Berlin, Humboldt Universität zu Berlin, and Berlin Institute of Health, Berlin; Cluster of Excellence NeuroCure (AH), Charité Universitätsmedizin Berlin, Berlin; Bernstein Center for Computational Neuroscience (AH, FS), Berlin; Max Planck Institute for Human Cognitive and Brain Sciences (LD, FS), Leipzig; and Max Planck Institute for Metabolism Research (KES), Cologne, Germany; Max Planck UCL Centre for Computational Psychiatry and Ageing Research (LD, CM) and Wellcome Centre for Human Neuroimaging (LD, CM, KES), Institute of Neurology, University College London, London, United Kingdom; Center for Social and Affective Neuroscience (RB), Linköping University, Linköping, Sweden; Scuola Internazionale Superiore di Studi Avanzati (CM), Trieste, Italy; Translational Neuromodeling Unit (CM, KES), Institute for Biomedical Engineering, University of Zurich and ETH Zurich, Zurich, Switzerland.

LD and RB contributed equally to this work.

Address correspondence to Lorenz Deserno, M.D., Max Planck UCL Centre for Computational Psychiatry and Ageing Research, London, 10-12 Russell Square, London WC1B 5EH, United Kingdom; E-mail: l.deserno@ucl.ac.uk.

Received Jul 24, 2019; revised Sep 11, 2019; accepted Oct 6, 2019.

Supplementary material cited in this article is available online at https://doi.org/10.1016/j.bpsc.2019.10.007.

REFERENCES

1. Bowie CR, Leung WW, Reichenberg A, McClure MM, Patterson TL, Heaton RK, *et al.* (2008): Predicting schizophrenia patients' real-world behavior with specific neuropsychological and functional capacity measures. Biol Psychiatry 63:505–511.
2. Green MF (1996): What are the functional consequences of neurocognitive deficits in schizophrenia? Am J Psychiatry 153:321–330.
3. Nuechterlein KH, Subotnik KL, Green MF, Ventura J, Asarnow RF, Gitlin MJ, *et al.* (2011): Neurocognitive predictors of work outcome in recent-onset schizophrenia. Schizophr Bull 37(suppl 2):S33–S40.
4. Gonzalez-Ortega I, de Los Mozos V, Echeburua E, Mezo M, Besga A, Ruiz de Azua S, *et al.* (2013): Working memory as a predictor of negative symptoms and functional outcome in first episode psychosis. Psychiatry Res 206:8–16.
5. Dominguez Mde G, Viechtbauer W, Simons CJ, van Os J, Krabbendam L (2009): Are psychotic psychopathology and neurocognition orthogonal? A systematic review of their associations. Psychol Bull 135:157–171.
6. Gold JM, Waltz JA, Prentice KJ, Morris SE, Heerey EA (2008): Reward processing in schizophrenia: A deficit in the representation of value. Schizophr Bull 34:835–847.
7. Barch DM, Dowd EC (2010): Goal representations and motivational drive in schizophrenia: The role of prefrontal-striatal interactions. Schizophr Bull 36:919–934.
8. Murray GK, Cheng F, Clark L, Barnett JH, Blackwell AD, Fletcher PC, *et al.* (2008): Reinforcement and reversal learning in first-episode psychosis. Schizophr Bull 34:848–855.
9. Leeson VC, Robbins TW, Matheson E, Hutton SB, Ron MA, Barnes TR, *et al.* (2009): Discrimination learning, reversal, and set-shifting in first-episode schizophrenia: Stability over six years and specific associations with medication type and disorganization syndrome. Biol Psychiatry 66:586–593.
10. Ragland JD, Cohen NJ, Cools R, Frank MJ, Hannula DE, Ranganath C (2012): CNTRICS imaging biomarkers final task selection: Long-term memory and reinforcement learning. Schizophr Bull 38:62–72.
11. Cools R, Clark L, Owen AM, Robbins TW (2002): Defining the neural mechanisms of probabilistic reversal learning using event-related functional magnetic resonance imaging. J Neurosci 22:4563–4567.
12. Waltz JA, Gold JM (2007): Probabilistic reversal learning impairments in schizophrenia: Further evidence of orbitofrontal dysfunction. Schizophr Res 93:296–303.
13. Waltz JA, Kasanova Z, Ross TJ, Salmeron BJ, McMahon RP, Gold JM, *et al.* (2013): The roles of reward, default, and executive control networks in set-shifting impairments in schizophrenia. PLoS One 8: e57257.
14. Culbreth AJ, Gold JM, Cools R, Barch DM (2016): Impaired activation in cognitive control regions predicts reversal learning in schizophrenia. Schizophr Bull 42:484–493.

15. Culbreth AJ, Westbrook A, Xu Z, Barch DM, Waltz JA (2016): Intact ventral striatal prediction error signaling in medicated schizophrenia patients. Biol Psychiatry Cogn Neurosci Neuroimaging 1:474–483.
16. Reddy LF, Waltz JA, Green MF, Wynn JK, Horan WP (2016): Probabilistic reversal learning in schizophrenia: Stability of deficits and potential causal mechanisms. Schizophr Bull 42:942–951.
17. Schlagenhauf F, Huys QJ, Deserno L, Rapp MA, Beck A, Heinze HJ, *et al.* (2014): Striatal dysfunction during reversal learning in unmedicated schizophrenia patients. NeuroImage 89:171–180.
18. Deserno L, Boehme R, Heinz A, Schlagenhauf F (2013): Reinforcement learning and dopamine in schizophrenia: Dimensions of symptoms or specific features of a disease group? Front Psychiatry 4:172.
19. Sutton RS, Barto AG (1998): Reinforcement Learning: An Introduction. Cambridge, MA: MIT Press.
20. Schultz W, Dayan P, Montague PR (1997): A neural substrate of prediction and reward. Science 275:1593–1599.
21. Steinberg EE, Keiflin R, Boivin JR, Witten IB, Deisseroth K, Janak PH (2013): A causal link between prediction errors, dopamine neurons and learning. Nat Neurosci 16:966–973.
22. Howes OD, Kambeitz J, Kim E, Stahl D, Slifstein M, Abi-Dargham A, *et al.* (2012): The nature of dopamine dysfunction in schizophrenia and what this means for treatment. Arch Gen Psychiatry 69:776–786.
23. Heinz A (2002): Dopaminergic dysfunction in alcoholism and schizophrenia—Psychopathological and behavioral correlates. Eur Psychiatry 17:9–16.
24. Maia TV, Frank MJ (2017): An integrative perspective on the role of dopamine in schizophrenia. Biol Psychiatry 81:52–66.
25. Deserno L, Heinz A, Schlagenhauf F (2017): Computational approaches to schizophrenia: A perspective on negative symptoms. Schizophr Res 186:46–54.
26. Rao RP, Ballard DH (1999): Predictive coding in the visual cortex: A functional interpretation of some extra-classical receptive-field effects. Nat Neurosci 2:79–87.
27. Stephan KE, Friston KJ, Frith CD (2009): Dysconnection in schizophrenia: From abnormal synaptic plasticity to failures of self-monitoring. Schizophr Bull 35:509–527.
28. Corlett PR, Frith CD, Fletcher PC (2009): From drugs to deprivation: A Bayesian framework for understanding models of psychosis. Psychopharmacology (Berl) 206:515–530.
29. Adams RA, Huys QJ, Roiser JP (2016): Computational psychiatry: Towards a mathematically informed understanding of mental illness. J Neurol Neurosurg Psychiatry 87:53–63.
30. Fletcher PC, Frith CD (2009): Perceiving is believing: A Bayesian approach to explaining the positive symptoms of schizophrenia. Nat Rev Neurosci 10:48–58.
31. Powers AR, Mathys C, Corlett PR (2017): Pavlovian conditioning-induced hallucinations result from overweighting of perceptual priors. Science 357:596–600.
32. Rushworth MF, Behrens TE (2008): Choice, uncertainty and value in prefrontal and cingulate cortex. Nat Neurosci 11:389–397.
33. Juckel G, Schlagenhauf F, Koslowski M, Wustenberg T, Villringer A, Knutson B, *et al.* (2006): Dysfunction of ventral striatal reward prediction in schizophrenia. NeuroImage 29:409–416.
34. Schlagenhauf F, Sterzer P, Schmack K, Ballmaier M, Rapp M, Wrase J, *et al.* (2009): Reward feedback alterations in unmedicated schizophrenia patients: Relevance for delusions. Biol Psychiatry 65:1032–1039.
35. Radua J, Schmidt A, Borgwardt S, Heinz A, Schlagenhauf F, McGuire P, Fusar-Poli P (2015): Ventral striatal activation during reward processing in psychosis: A neurofunctional meta-analysis. JAMA Psychiatry 72:1243–1251.
36. Dowd EC, Frank MJ, Collins A, Gold JM, Barch DM (2016): Probabilistic reinforcement learning in patients with schizophrenia: Relationships to anhedonia and avolition. Biol Psychiatry Cogn Neurosci Neuroimaging 1:460–473.
37. Behrens TE, Woolrich MW, Walton ME, Rushworth MF (2007): Learning the value of information in an uncertain world. Nat Neurosci 10:1214–1221.
38. Iglesias S, Mathys C, Brodersen KH, Kasper L, Piccirelli M, den Ouden HE, *et al.* (2013): Hierarchical prediction errors in midbrain and basal forebrain during sensory learning. Neuron 80:519–530.
39. Rushworth MF, Noonan MP, Boorman ED, Walton ME, Behrens TE (2011): Frontal cortex and reward-guided learning and decision-making. Neuron 70:1054–1069.
40. Mathys C, Daunizeau J, Friston KJ, Stephan KE (2011): A Bayesian foundation for individual learning under uncertainty. Front Hum Neurosci 5:39.
41. Mathys CD, Lomakina EI, Daunizeau J, Iglesias S, Brodersen KH, Friston KJ, *et al.* (2014): Uncertainty in perception and the hierarchical Gaussian filter. Front Hum Neurosci 8:825.
42. Boehme R, Deserno L, Gleich T, Katthagen T, Pankow A, Behr J, *et al.* (2015): Aberrant salience is related to reduced reinforcement learning signals and elevated dopamine synthesis capacity in healthy adults. J Neurosci 35:10103–10111.
43. Reiter AMF, Deserno L, Kallert T, Heinze HJ, Heinz A, Schlagenhauf F (2016): Behavioral and neural signatures of reduced updating of alternative options in alcohol-dependent patients during flexible decision-making. J Neurosci 36:10935–10948.
44. Reiter AMF, Heinze HJ, Schlagenhauf F, Deserno L (2017): Impaired flexible reward-based decision-making in binge eating disorder: Evidence from computational modeling and functional neuroimaging. Neuropsychopharmacology 42:628–637.
45. Stephan KE, Penny WD, Daunizeau J, Moran RJ, Friston KJ (2009): Bayesian model selection for group studies. NeuroImage 46:1004–1017.
46. Rigoux L, Stephan KE, Friston KJ, Daunizeau J (2014): Bayesian model selection for group studies—revisited. NeuroImage 84:971–985.
47. Stephan KE, Schlagenhauf F, Huys QJ, Raman S, Aponte EA, Brodersen KH, *et al.* (2017): Computational neuroimaging strategies for single patient predictions. NeuroImage 145:180–199.
48. Kaplan CM, Saha D, Molina JL, Hockeimer WD, Postell EM, Apud JA, *et al.* (2016): Estimating changing contexts in schizophrenia. Brain 139:2082–2095.
49. Vinckier F, Gaillard R, Palminteri S, Rigoux L, Salvador A, Fornito A, *et al.* (2016): Confidence and psychosis: A neuro-computational account of contingency learning disruption by NMDA blockade. Mol Psychiatry 21:946–955.
50. Krystal JH, Perry EB Jr, Gueorguieva R, Belger A, Madonick SH, Abi-Dargham A, *et al.* (2005): Comparative and interactive human psychopharmacologic effects of ketamine and amphetamine: Implications for glutamatergic and dopaminergic model psychoses and cognitive function. Arch Gen Psychiatry 62:985–994.
51. Lewis DA, Gonzalez-Burgos G (2006): Pathophysiologically based treatment interventions in schizophrenia. Nat Med 12:1016–1022.
52. Durstewitz D, Seamans JK (2008): The dual-state theory of prefrontal cortex dopamine function with relevance to catechol-*o*-methyltransferase genotypes and schizophrenia. Biol Psychiatry 64:739–749.
53. McTeague LM, Huemer J, Carreon DM, Jiang Y, Eickhoff SB, Etkin A (2017): Identification of common neural circuit disruptions in cognitive control across psychiatric disorders. Am J Psychiatry 174:676–685.
54. Glahn DC, Ragland JD, Abramoff A, Barrett J, Laird AR, Bearden CE, *et al.* (2005): Beyond hypofrontality: A quantitative meta-analysis of functional neuroimaging studies of working memory in schizophrenia. Hum Brain Mapp 25:60–69.
55. Sterzer P, Adams RA, Fletcher P, Frith C, Lawrie SM, Muckli L, *et al.* (2018): The predictive coding account of psychosis. Biol Psychiatry 84:634–643.
56. Reinen JM, Van Snellenberg JX, Horga G, Abi-Dargham A, Daw ND, Shohamy D (2016): Motivational context modulates prediction error response in schizophrenia. Schizophr Bull 42:1467–1475.
57. Nielsen MO, Rostrup E, Wulff S, Bak N, Broberg BV, Lublin H, *et al.* (2012): Improvement of brain reward abnormalities by antipsychotic monotherapy in schizophrenia. Arch Gen Psychiatry 69:1195–1204.
58. Schlagenhauf F, Juckel G, Koslowski M, Kahnt T, Knutson B, Dembler T, *et al.* (2008): Reward system activation in schizophrenic patients switched from typical neuroleptics to olanzapine. Psychopharmacology (Berl) 196:673–684.

59. Stephan KE, Bach DR, Fletcher PC, Flint J, Frank MJ, Friston KJ, *et al.* (2016): Charting the landscape of priority problems in psychiatry, part 1: Classification and diagnosis. Lancet Psychiatry 3:77–83.
60. Stephan KE, Penny WD, Moran RJ, den Ouden HE, Daunizeau J, Friston KJ (2010): Ten simple rules for dynamic causal modeling. NeuroImage 49:3099–3109.
61. Penny WD, Stephan KE, Daunizeau J, Rosa MJ, Friston KJ, Schofield TM, *et al.* (2010): Comparing families of dynamic causal models. PLoS Comput Biol 6:e1000709.
62. Cullen M, Davey B, Friston KJ, Moran RJ (2018): Active inference in OpenAI Gym: A paradigm for computational investigations into psychiatric illness. Biol Psychiatry Cogn Neurosci Neuroimaging 3:809–818.
63. Brodersen KH, Deserno L, Schlagenhauf F, Lin Z, Penny WD, Buhmann JM, *et al.* (2014): Dissecting psychiatric spectrum disorders by generative embedding. NeuroImage Clin 4:98–111.
64. Wolfers T, Doan NT, Kaufmann T, Alnaes D, Moberget T, Agartz I, *et al.* (2018): Mapping the heterogeneous phenotype of schizophrenia and bipolar disorder using normative models. JAMA Psychiatry 75:1146–1155.
65. Huys QJ, Maia TV, Frank MJ (2016): Computational psychiatry as a bridge from neuroscience to clinical applications. Nat Neurosci 19:404–413.
66. Stephan KE, Mathys C (2014): Computational approaches to psychiatry. Curr Opin Neurobiol 25:85–92.
67. Heinz A (2017): A New Understanding of Mental Disorders: Computational Models for Dimensional Psychiatry. Cambridge, MA: MIT Press.